

# Tetragonal CuO: A new end member of the 3d transition metal monoxides

Wolter Siemons,<sup>1,2</sup> Gertjan Koster,<sup>1,2</sup> Dave H. A. Blank,<sup>1</sup> Robert  
H. Hammond,<sup>2</sup> Theodore H. Geballe,<sup>2</sup> and Malcolm R. Beasley<sup>2</sup>

<sup>1</sup>*Faculty of Science and Technology and MESA+ Institute for Nanotechnology,  
University of Twente, 7500 AE Enschede, The Netherlands*

<sup>2</sup>*Geballe Laboratory for Advanced Materials,  
Stanford University, Stanford, California 94305, USA*

## Abstract

Monoclinic CuO is anomalous both structurally as well as electronically in the 3d transition metal oxide series. All the others have the cubic rock salt structure. Here we report the synthesis and electronic property determination of a tetragonal (elongated rock salt) form of CuO created using an epitaxial thin film deposition approach. In situ photoelectron spectroscopy suggests an enhanced charge transfer gap  $\Delta$  with the overall bonding more ionic. As an end member of the 3d transition monoxides, its magnetic properties should be that of a high  $T_N$  antiferromagnet.

PACS numbers:

## INTRODUCTION

Since the discovery of high temperature superconductivity in the copper oxide perovskites, its origin and mechanism are still unexplained and under debate. The original proposal by Bednorz and Mueller<sup>1</sup> and others, that a Jahn-Teller distortion in a highly symmetric divalent copper monoxide structure introducing a strong electron-phonon interaction causes superconductivity, has led to extensive studies toward the synthesis of the family of cuprates. The simplest form, the cubic rock salt copper monoxide, however, has not been found in nature nor has been successfully synthesized, yet. CuO is the exceptional member of the rock salt series as one traverses the periodic table from MnO to CuO. It deviates substantially from the trends exhibited by the members with lower atomic number. All the others have the cubic rock salt structure and all are correlated antiferromagnetic insulators.<sup>2,3,4,5</sup> CuO differs in having a monoclinic structure as opposed to the rock salt structure of the other monoxides, and, as shown in Fig. 1, it also has a substantially lower Néel temperature than a simple extrapolation of the trend across the periodic table would suggest. Presumably, this exceptional behavior is a consequence of its lower symmetry structure. Clearly, the properties of CuO in higher symmetry structures would be of great fundamental interest in understanding correlated materials.<sup>6,7</sup> Here we report the synthesis and preliminary electronic property determination of a tetragonal (elongated rock salt, displayed in Fig. 1b) form of CuO created for the first time, by using an epitaxial thin film deposition approach. The results demonstrate that higher symmetry phases of this important correlated oxide are possible and now available for physical studies. Looking ahead, if the trend shown in Fig 1a were followed, the Néel temperature of rock salt CuO would be very high (700 to 800 K), as would be its associated exchange coupling  $J$ . If such a high- $J$  CuO could be doped, its properties would be of great interest in the context of the earlier mentioned high- $T_c$  superconductors.

The films discussed in this work have been well characterized from the structural point of view using reflection high energy electron diffraction (RHEED) and x-ray photoemission diffraction (XPD), and from the electronic structure point of view using in-situ x-ray and ultraviolet photoemission spectroscopy ((XPS/UPS). As we will discuss below, by comparing with the stable copper oxides, we have determined the Cu has a charge of +2 and that the tetragonal structure is more ionic than the monoclinic phase. Preliminary attempts to dope our films using charge transfer from over-layers have also been carried out. Taken together, the results demonstrate that higher symmetry forms of this important correlated oxide are possible and available for physical study.

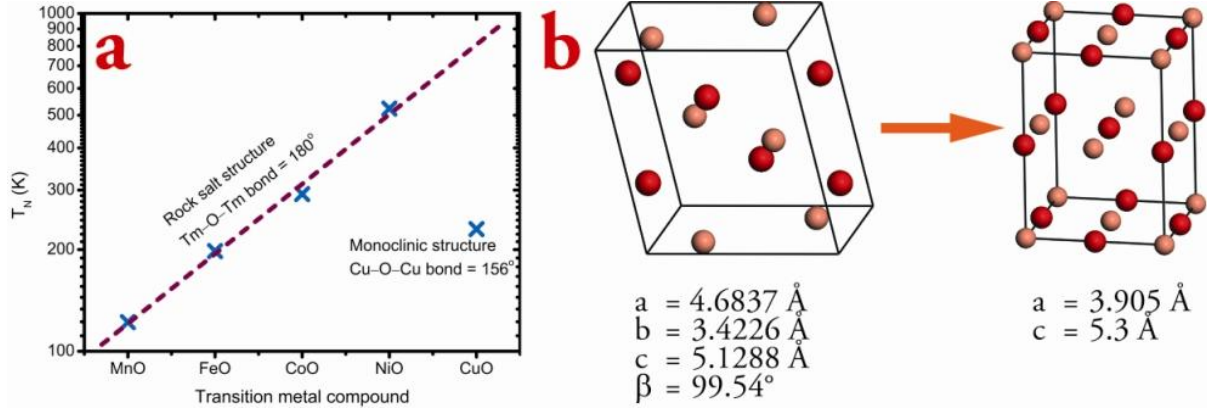


FIG. 1: (a) An overview of the Néel temperatures for transition metal monoxides with a rock salt structure.  $T_N$  increases exponentially with each element up to NiO as indicated by the dashed line, which is a fit of the first four points. The  $T_N$  of the monoclinic CuO structure does not follow this trend, but is much lower, possibly due to a change in the Tm–O–Tm bond angle. When a rocksalt structure of CuO is formed  $T_N$  might follow the trend and linear extrapolation predicts a  $T_N$  slightly higher than 800 K. (b) The change in unit cell symmetry going from bulk (monoclinic) to the strained unit cell on SrTiO<sub>3</sub> (tetragonal), including the unit cell parameters. The lighter colored atoms represent oxygen and the darker colored atoms the copper.

## SYNTHESIS AND ANALYSIS

Our epitaxial films of tetragonal CuO were grown in a UHV chamber on SrTiO<sub>3</sub> substrates using pulsed laser deposition (PLD), although we have also grown sample using electron beam evaporation. For PLD a Lambda Physic LPX 210 KrF excimer laser produces a 248 nm wavelength beam with a typical pulse length of 20–30 ns. A rectangular mask shapes the beam selecting only the homogeneous part, and a variable attenuator permits variation of the pulse energy. The variable attenuator also offers the possibility to run the laser at the same voltage every run, which ensures the same pulse shape every time and therefore the best reproducibility. A lens makes an image of the mask on the target resulting in a well defined illuminated area. Energy density on the target was kept at  $2.1 \text{ J cm}^{-2}$  with a repetition rate of 1 Hz. The temperature of the substrate was fixed to 600 °C. Atomic oxygen was provided during deposition by a microwave plasma source (Astex SXRHA) with the source operating at 600 W with a flow of 2.5 sccm oxygen, resulting in a background deposition pressure in the system of  $1.5 \times 10^{-5}$  Torr and an estimated  $3 \times 10^{17}$  oxygen atoms  $\text{cm}^{-2} \text{ s}^{-1}$ .<sup>8</sup> The growth was monitored by RHEED.

Films were grown on either insulating or conducting (0.5% Nb doped) SrTiO<sub>3</sub>. The latter offers

the advantage of reduced charging when performing photoemission spectroscopy (PES) on the insulating CuO samples. Both types of substrates were TiO<sub>2</sub> terminated, as described by Koster and coworkers.<sup>9</sup> In order to stabilize the new phase, it is of utmost importance to oxidize Cu to a 2+ state. This was accomplished by using a target of CuO and providing atomic oxygen during deposition.

After deposition samples were cooled down in atomic oxygen. The films were typically unstable in atomic oxygen below 300 °C. Specifically, it was found that the films would relax to tenorite when cooled to room temperature under deposition conditions. To avoid this problem, the atomic oxygen was switched off at 300 °C and the sample then cooled to room temperature in molecular oxygen ( $\sim 10^{-5}$  Torr). These results imply that the stability line for the epitaxially stabilized tetragonal CuO when exposed to atomic oxygen lies around 300 °C.

The thickness of the tetragonal CuO samples is limited by a relaxation to the tenorite phase above a certain thickness. For most samples 300 laser pulses were used in the PLD process to guarantee a streaky RHEED pattern with no 3D spots. This corresponds to a layer thickness between 15 and 20 Å as determined with x-ray reflectivity and angle resolved XPS measurements.<sup>10</sup> AFM imaging confirms that thin samples are flat with the SrTiO<sub>3</sub> step structure still visible, whereas the samples that are thicker exhibit islands on top, associated with the film growth process, that cause the observed 3D RHEED pattern.

Let us note here, that after exposure to air the top layer of the CuO was found to degrade to tenorite, whereas the layer closest to the interface with SrTiO<sub>3</sub> is found to be mostly tetragonal. This result could be established using angle dependent XPS, as discussed in detail in the thesis by Siemons.<sup>11</sup> Also, when a sample is kept under vacuum after growth, the CuO is slowly reduced over a period of days.<sup>12</sup> After four days the intensity of the satellite peaks are reduced to about half their size after deposition. All XPS spectra are referenced with respect to the Ti 2*p* peak of the substrate.

The XPS and UPS measurements are performed *in situ* with a VG scientific ESCA lab Mark II system. The photon source for XPS is Al *k*α and for UPS measurements HeI (21.2 eV) radiation was used. Both sources are non-monochromatic and spectra are corrected for satellites by use of software.

## INITIAL GROWTH

When grown on doubly terminated substrates, the growth was found to be more 3D, and the films relaxed to the tenorite phase at an earlier stage in the deposition. Similar results were observed on other substrate materials, such as DyScO<sub>3</sub> and LaAlO<sub>3</sub>, where 3D growth patterns of the relaxed structure would occur at a very early stage. Due to the polar nature of these materials those substrates are either doubly terminated (a reliable method to make them singly terminated such as with SrTiO<sub>3</sub> has not been fully developed), or complicates the layer-by-layer growth of a neutral material such as CuO<sup>13</sup>. In addition, these other substrates have different lattice parameters as well, which might affect their efficacy for epitaxy of CuO.

Fig. 2a–c show the evolution of the RHEED pattern in the case of successful growth of the tetragonal phase. Specifically, a streaky pattern, which is 4-fold symmetric when the sample is rotated around the surface normal, emerges during deposition, without any 3D spots between the streaks. In contrast, Fig. 2d shows the RHEED pattern that emerges when the film relaxes to the tenorite phase. It is clearly different from that of the new tetragonal phase. Such a streaky pattern was observed before for the growth of CuO on MgO,<sup>14</sup> but no different symmetry of the CuO unit cell was observed in that work.

## DETERMINING LATTICE PARAMETERS

To determine the in-plane lattice parameters of the new phase, RHEED spectra were used. Spectra taken along the SrTiO<sub>3</sub> (10) and (11) are shown in figure 3. Since the lattice parameters of the SrTiO<sub>3</sub> are well known (3.905 Å cubic), the lattice parameters of CuO can be calculated by comparing its lines to those of SrTiO<sub>3</sub>. There is a subtlety here, however. One must correctly identify the lines. For a rock salt structure, not all the diffraction peaks are allowed, and those that are allowed are different in 2D and 3D. We find that for our very thin films the 2D result is required. Specifically, in 2D the structure factor becomes:

$$\text{h,k unmixed: } F_{hk} = 2 \sum_{n/2} f_n e^{2\pi i(hx_n + ky_n)}$$

$$\text{h,k mixed: } F_{hk} = 0$$

Therefore, in the 2D case, the (01) reflection is not allowed but the (11) is, and it follows that the shortest spacing between the RHEED lines corresponds to the (11) reflection. On the other hand,

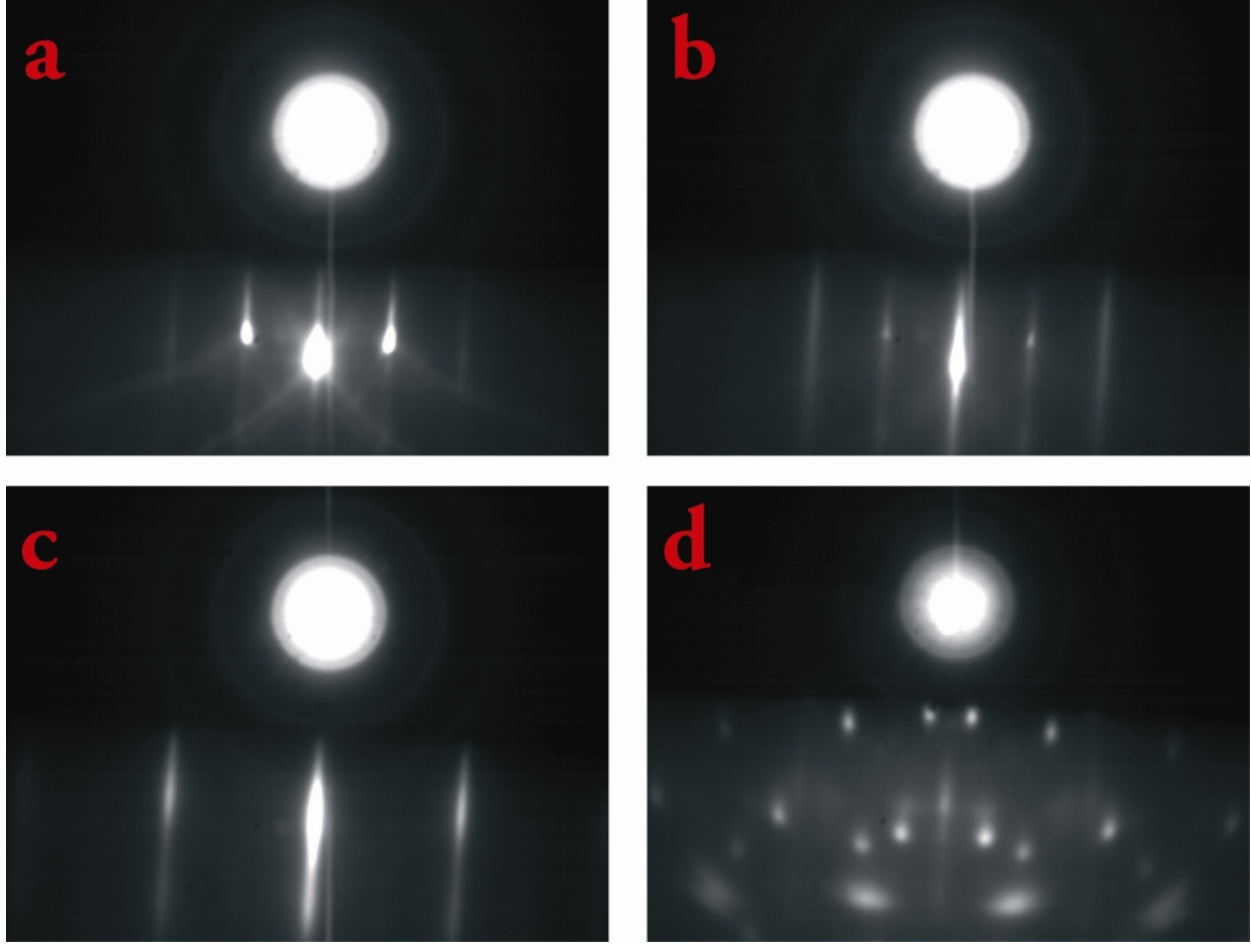


FIG. 2: (a-c) The evolution of the RHEED spectrum during the growth of CuO on SrTiO<sub>3</sub> taken along the (01) direction of SrTiO<sub>3</sub> shows a transition from a clear 2D pattern for bare SrTiO<sub>3</sub> (a) to the streaky pattern of CuO (c). (d) When growth is continued the film relaxes to tenorite showing clear 3D spots.

if the pattern were 3D, the shortest spacing would correspond to the (01) reflection. Analysis of the data assuming such an identification leads to non-physical results.

With the dimensionality established, it is straightforward to determine the lattice constants. In the (11) direction of the SrTiO<sub>3</sub> substrate, the (11) and (22) reflections of CuO are allowed, and along the (01) direction of the SrTiO<sub>3</sub>, the (02) and (04) reflections of CuO are allowed. The CuO in-plane lattice parameters are exactly the same size as the SrTiO<sub>3</sub> underneath. This corresponds to a Cu–O bond length of 1.95 Å in-plane, a number which corresponds well with values found in high T<sub>c</sub> materials or in monoclinic CuO. If the unit cell were cubic this would result in a unit cell volume of 59.5 Å<sup>3</sup>, too far from the 81.1 Å<sup>3</sup> of tenorite to be physically reasonable. We conclude, therefore, that the unit cell must be elongated along the out-of-plane direction. But based on the

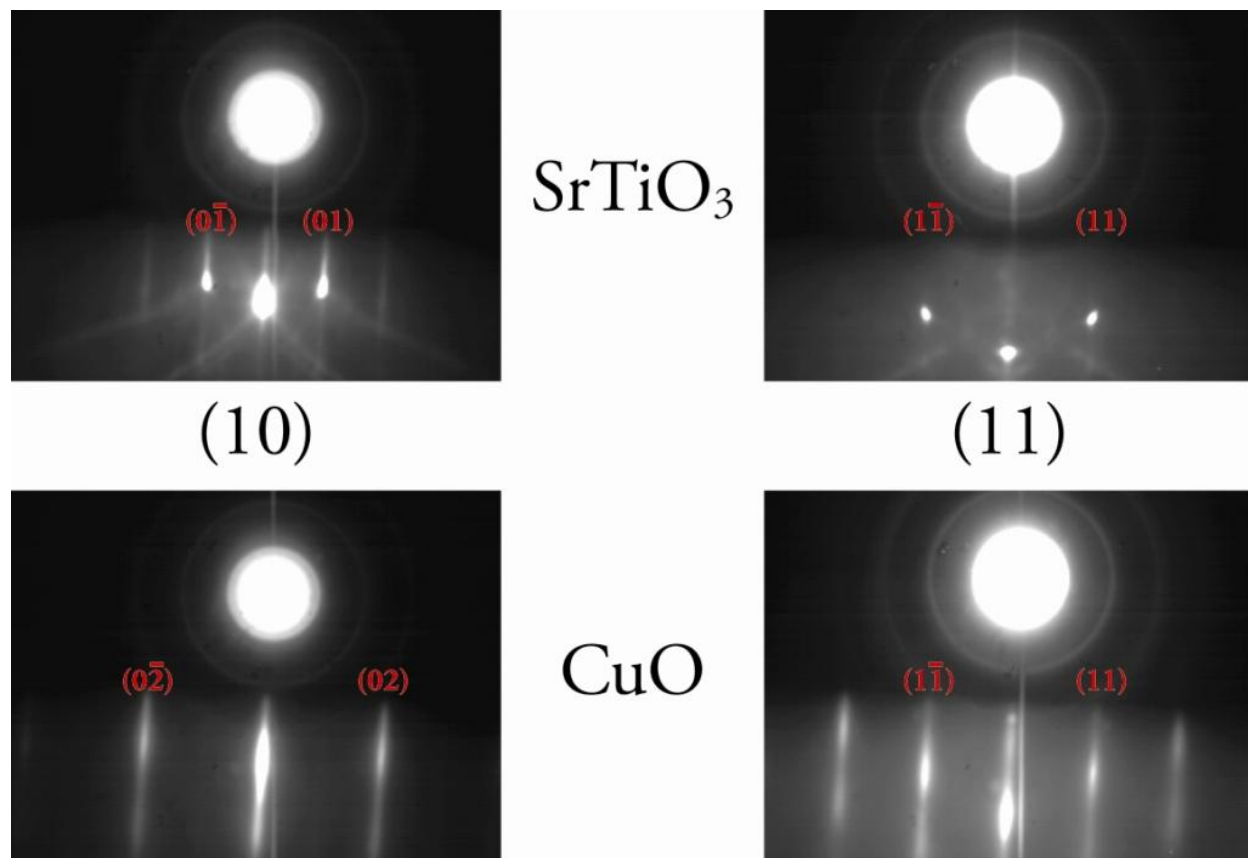


FIG. 3: The electron diffraction patterns of  $\text{SrTiO}_3$  and  $\text{CuO}$  taken along their (10) and (11) directions. Even though the (10) reflection of  $\text{CuO}$  is not allowed as explained in the text, very faint lines at its position are usually visible. The patterns shown here are both fourfold symmetric when the sample is rotated around its azimuthal axis.

RHEED spectra alone, we cannot draw conclusions about the out-of-plane lattice constant.

To measure the out-of-plane lattice constant, we employed XPD. To verify that the technique would produce reliable results, it was first applied to a conducting Nb-doped  $\text{SrTiO}_3$  substrate. Simulations and measurements were strikingly similar. Two energies were measured: the O 1s and the Cu 2p. For the oxygen signal, a contribution of the substrate is to be expected, since the escape depth of the electrons is of the order of the thickness of the  $\text{CuO}$  layer. The copper signal, on the other hand, comes solely from the film because the substrate contains no copper. The copper pattern shows a fourfold symmetry as shown on the right in figure 4, which is indicative of a fourfold symmetric unit cell, such as a rock salt structure. By comparing simulations and measurements the c-axis length of the unit cell was determined to be 5.3 Å. Using the XPD data, the out-of-plane lattice parameter cannot be determined more accurately. These lattice parameters

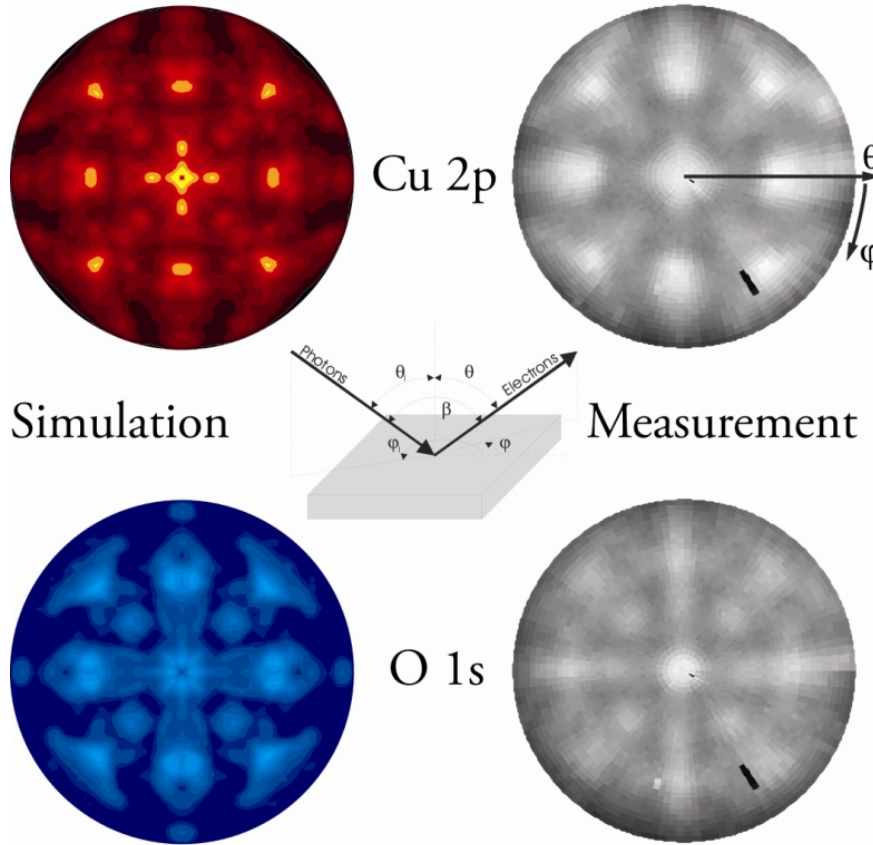


FIG. 4: XPD patterns for CuO measured (on the right) at two binding energies: the O 1s and the Cu  $2p_{3/2}$  main line. The measurements were performed with the pass energy set at 100 eV, an acceptance angle of 5 degrees in steps of  $2^\circ$  for  $\theta$  ( $90-30^\circ$ ) and  $3^\circ$  for  $\phi$  ( $0-360^\circ$ ). Simulations of the CuO in tetragonal form are shown on the left, as calculated with software by Abajo *et al.*<sup>15</sup> The Cu signal comes solely from the film, whereas the O signal has a contribution from the substrate. The Cu pattern shows clear four-fold symmetry, which is not what would be expected from a single domain tenorite film.

are also shown in Fig. 1b. Note that the films described in this work typically are 3 – 4 unit cells thick.

With this complete set of unit cell dimensions, the unit cell volume now becomes  $81.1 \text{ \AA}^3$ , which is the same as for tenorite and physically reasonable. The shortest Cu–O bond length in this structure is  $1.95 \text{ \AA}$ , which corresponds to the value found in tenorite. The shortest Cu–Cu and O–O bond lengths are  $2.76 \text{ \AA}$ , a value that is in between the values found for the two in tenorite.



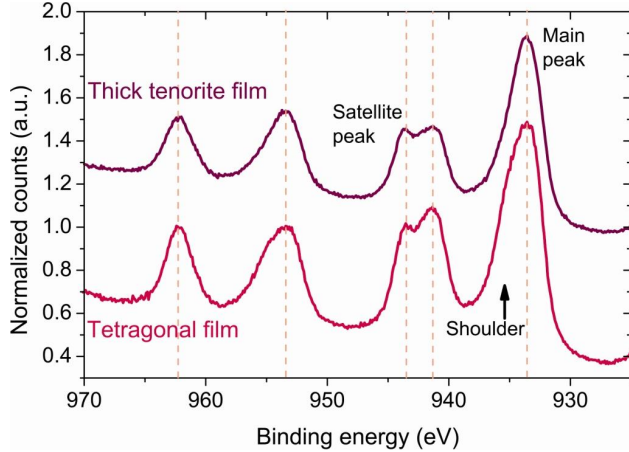


FIG. 5: The Cu  $2p$  core level XPS spectrum of the tetragonal CuO looks significantly different from the tenorite spectrum. The most striking differences are the broadening of the main peak, the narrowing of the satellite peak, and the redistribution of weight in the satellite peak. The spectra have been normalized on the  $2p_{1/2}$  peak and the tenorite spectrum has been given an offset for clarity.

## ELECTRONIC STRUCTURE

Let us now turn to the electronic structure of this new phase of CuO. The XPS spectra of the Cu  $2p$  lines for the thin tetragonal epitaxial films as well as those for thicker films in the tenorite structure are shown in Fig. 5. For tenorite, we find 933.5 eV for the binding energy of the Cu  $2p_{3/2}$  and 529.4 eV for the O  $1s$ . These correspond well to the values found in literature. For our new tetragonal phase, the energies of these lines do not appear to change significantly. On the other hand, compared to the tenorite spectrum, the tetragonal CuO spectrum has a larger shoulder on the main peak at higher binding energy, a narrower satellite peak, and the spectral weight of the first satellite peak has shifted to lower binding energy. More precisely, when going from the monoclinic to the tetragonal phase the full width at half maximum (fwhm) of the main peak increases from 3.6 to 4.1 eV, whereas the fwhm of the satellite peak decreases from 4.5 to 4.2 eV.

The valence band spectrum was measured with He I radiation, and the results are presented in figure 6, together with a representative spectrum of tenorite, taken by Warren et al.<sup>16</sup> For the tenorite phase, the spectrum is representative to that obtained by other groups.<sup>12,16,17,18,19</sup> For example, there are no states at the Fermi level, which is as expected for an insulator.

Comparing the spectra for tenorite and our CuO, there are some notable differences. The peak at low binding energy ( $\sim 1.9$  eV), which is caused by both oxygen and copper orbitals,<sup>20</sup> is not as

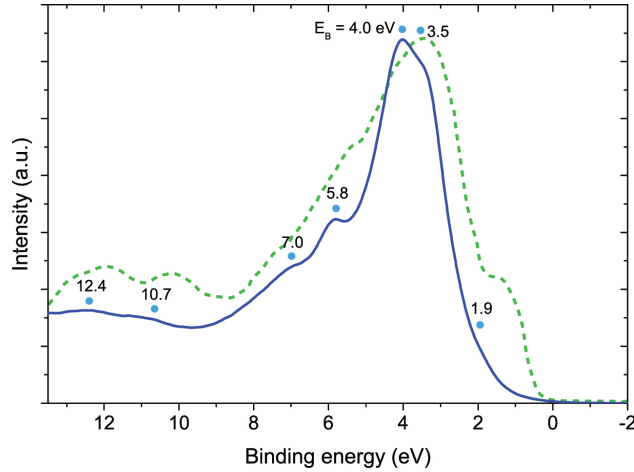


FIG. 6: The tetragonal CuO valence band spectrum, solid blue line, measured with HeI radiation and the peak positions indicated with cyan dots. The Nb doped SrTiO<sub>3</sub> substrate contributes to the spectrum for such thin films, but its contribution is expected to be very small. The dotted line is a typical tenorite spectrum taken at 70 eV radiation, by Warren et al.<sup>16</sup>

strong in our spectrum as it is in the spectra of tenorite. Also the largest peak, mainly belonging to copper, clearly consists of two separate peaks in our spectrum, and is not observed before for tenorite. Note that calculations on the tenorite band structure show a splitting of this peak<sup>17,20</sup>, and in some measurements a shoulder is visible.<sup>18</sup> The peaks at 5.8 and 7.0 eV are both oxygen peaks and are also predicted by calculations.<sup>20</sup> The double peak feature at higher energy (10–13 eV) is a copper feature only predicted by the most advanced calculations.<sup>19,20,21</sup> All calculations on tenorite predict the peaks to be at lower binding energies than measured here, and the spectrum we observe is shifted up by as much as 2 eV. The spectrum for the tetragonal phase is shifted to higher binding energies by about 0.5 eV compared to the tenorite phase. Speculatively, assuming that the Fermi level is in the middle of the gap, this would imply a larger charge transfer gap  $\Delta$ . For a film of this thickness, some contribution of the substrate to the spectrum is expected. SrTiO<sub>3</sub> has two large peaks at higher energies (4.4 and 6.6 eV), but no clear evidence of a contribution of these peaks and the measured spectrum has been found.

## INITIAL DOPING EXPERIMENTS

As mentioned in the introduction, we have made some preliminary attempts to dope our new tetragonal form of CuO, which like the other transition metal monoxides, we expect to be a Mott

insulator of the charge-transfer type.<sup>22,23</sup> To attempt charge transfer doping, without breaking vacuum, alkali metals were deposited on top of our tetragonal CuO films. Alkali metals were chosen because their outer electrons are very weakly bound and would be expected to be transferred into the CuO. This property also makes them very reactive, and so we have not attempted analyzing these samples outside our deposition chamber. Of course, even if charge is transferred the question remains whether the charges will be mobile or localized. A capability to measure the transport properties of our samples without leaving the UHV environment is under development.

Two alkali metals were used: Li and Cs. The XPS results of one of the charge transfer doping experiments using Cs are shown in Fig 7. Deposition was incremental, and after each deposition photoemission spectra were taken. The Cu  $2p$  spectra in 7 show a systematic change with increasing Cs coverage. The O  $1s$  peak at about 530 eV does not change significantly when Cs is deposited. The Cs peaks themselves are lower than one would expect for elemental Cs by about 1 eV. CsOH is 1.4 eV lower than Cs metal, and the lower binding energy therefore suggests that Cs has donated an electron. The spectral shift in the  $2p$  peaks can be explained by doping of the Cs electrons into the CuO: in a localized picture this would generate more  $\text{Cu}^{1+}$  at the expense of  $\text{Cu}^{2+}$  and make the spectrum look more like  $\text{Cu}_2\text{O}$ . On the other hand, a similar effect would be expected to occur if Cs removed oxygen from the CuO, which also creates more  $\text{Cu}^{1+}$ . In both cases, the CuO would be electron doped, but UPS measurements showed no Fermi edge, and some charging was observed during XPS measurements. Note that we used the Ti  $2p$  peak from the substrate as an internal energy reference. The Li doped samples showed a similar trend.

## DISCUSSION

The RHEED and XPD results seem unequivocal that a tetragonal structure of CuO has been synthesized, through the use of epitaxy. The more interesting question is what are the electronic properties of this higher symmetry phase. Comparison of our XPS results for the tetragonal form of CuO with those for tenorite reveals that the main peak becomes broader and the satellite peak sharper when the tetragonal phase is formed. The intensity distribution in the satellite peak shifts more to lower binding energies. According to Van Veenendaal and Sawatsky,<sup>24,25</sup> the width of the main peak is related to whether the screening electrons come from the closest ligand atoms or from ligand atoms further away. This would suggest that the screening electrons are more delocalized in the tetragonal structure. Note that while the shortest Cu–O bond lengths in the tetragonal structure

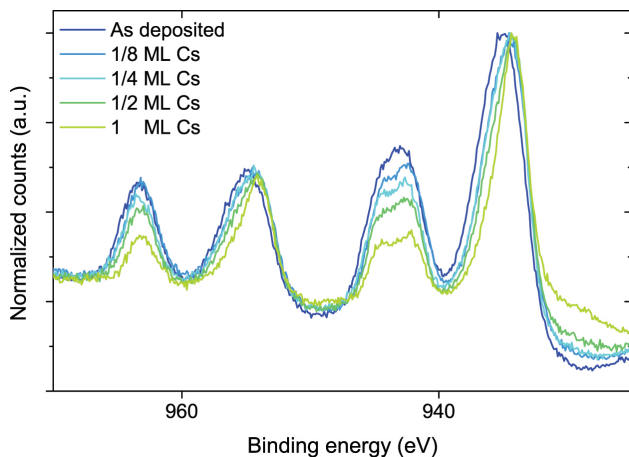


FIG. 7: XPS Cu  $2p$  spectrum of an as-deposited tetragonal CuO film and spectra taken after deposition of approximately  $\frac{1}{8}$ ,  $\frac{1}{4}$ ,  $\frac{1}{2}$ , and 1.0 MLs of Cs. The spectrum changes systematically towards a  $\text{Cu}^{1+}$  spectrum, which suggests charge carriers are created. The increase of the background at low binding energy is caused by a nearby Cs peak.

are similar to those in tenorite, there are also much longer bond lengths in the tetragonal structure, which might have an influence on the nature of the electrons. For the construction of the unit cell we have assumed all  $180^\circ$  Cu–O–Cu bonds, whereas they could be less due to Jahn-Teller distortions for example. Other measurements are required to accurately determine the bond angles, which are known to have a profound impact on especially the magnetic properties.

The structure of the satellite peak is harder to understand. The similarity with  $\text{CuCl}_2$  spectra from the literature is striking though.<sup>26</sup> Okada *et al.*<sup>27</sup> have performed extensive modeling of the satellite peak of  $\text{CuCl}_2$ . They argue that the shape of the satellite peak is mostly determined by the coupling-strength ratio between the  $\sigma$  and  $\pi$  bondings and the amount of hybridization of these states. Following their model suggests that the degree of hybridization is weaker in the tetragonal structure than in tenorite. In other words, the bonding in the tetragonal structure seems to have a more ionic character.

The UPS spectrum of tetragonal CuO is very similar to that measured for tenorite. Some notable differences include the intensity of the low energy peak, the splitting of the main peak, and a general shift of the spectrum to higher binding energies of about half an eV. Delocalized band calculations (local density approximation) performed for tenorite do not reproduce measurements on the tetragonal phase, suggesting the valence bands are changed with the structural change. Electron correlation effects are important in these materials, and neglecting them results in in-

complete DOS spectra and conducting ground states. The best predictions come from cluster calculations (configuration interaction (CI) calculations), which predict the entire spectrum accurately, but shifted to slightly lower binding energy. Eskes *et al.*<sup>21</sup> have investigated the nature of the first ionization state of CuO, which has either a triplet or a singlet character. The singlet state peak is the one closest to the Fermi level (1.9 eV in our spectrum) and the triplet state is the next one up (3.6 eV for this work). The energy difference between these peaks is closely related to the Cu–O distances, specifically the ratio between the Cu–O distance out-of-plane and in-plane, which is about 1.4 for the tetragonal unit cell. Based on their model we would expect to see an energy difference of 0.85 eV between the two peaks. The measured distance is much larger for reasons that are not well understood. An important next step in this research will be to specifically calculate the band structure for the tetragonal CuO.

## CONCLUSION

In conclusion, through the use of epitaxy, a nearly rock salt form of CuO has been synthesized that is now available for physical study. Preliminary electron structure studies suggest that the charge transfer gap  $\Delta$  is enhanced in the tetragonal phase and the overall bonding seems more ionic. As a new end member of the 3d transition monoxides, its magnetic properties should be that of a high  $T_N$  antiferromagnet.

This work supported by the DoE with additional support from EPRI. We would like to thank P.M. Grant for many useful conversations and his continuing interest in this work. We would also like to acknowledge W.A. Harrison and G.A. Sawatzky for useful conversations and A. Vailionis for critical help in understanding the RHEED patterns.

- 
1. J. Bednorz and K. Muller, *Reviews of Modern Physics* **60**, 585 (1988).
  2. L. F. Mattheiss, *Phys. Rev. B* **5**, 290 (1972).
  3. K. Terakura, T. Oguchi, A. R. Williams, and J. Kübler, *Phys. Rev. B* **30**, 4734 (1984).
  4. W. A. Harrison, *Physical Review B* **76**, 054417 (2007).
  5. J. Zaanen and G. A. Sawatzky, *Canadian Journal of Physics* **65**, 1262 (1987).
  6. A. Georges, G. Kotliar, W. Krauth, and M. J. Rozenberg, *Reviews of Modern Physics* **68**, 13 (1996).
  7. C. H. Ahn, J.-M. Triscone, and J. Mannhart, *Nature* **424**, 1015 (2003).

8. N. J. C. Ingle, R. H. Hammond, M. R. Beasley, and D. H. A. Blank, *Applied Physics Letters* **75**, 4162 (1999).
9. G. Koster, B. L. Kropman, G. J. H. M. Rijnders, D. H. A. Blank, and H. Rogalla, *Applied Physics Letters* **73**, 2920 (1998).
10. S. Spruytte, C. Coldren, J. Harris, D. Pantelidis, H.-J. Lee, J. Bravman, and M. Kelly, *Journal of Vacuum Science and Technology A: Vacuum, Surfaces, and Films* **19**, 603 (2001).
11. W. Siemons, Ph.D. thesis, University of Twente (2008).
12. Z.-X. Shen, R. S. List, D. S. Dessau, F. Parmigiani, A. J. Arko, R. Bartlett, B. O. Wells, I. Lindau, and W. E. Spicer, *Physical Review B* **42**, 8081 (1990).
13. N. Nakagawa, H. Hwang, and D. Muller, *Nature Materials* **5**, 204 (2006).
14. A. Catana, J.-P. Locquet, S. M. Paik, and I. K. Schuller, *Phys. Rev. B* **46**, 15477 (1992).
15. F. J. García de Abajo, M. A. Van Hove, and C. S. Fadley, *Physical Review B* **63**, 075404 (2001).
16. S. Warren, W. R. Flavell, A. G. Thomas, J. Hollingworth, P. L. Wincott, A. F. Prime, S. Downes, and C. Chen, *Journal of Physics: Condensed Matter* **11**, 5021 (1999).
17. J. Ghijsen, L. H. Tjeng, J. van Elp, H. Eskes, J. Westerink, G. A. Sawatzky, and M. T. Czyzyk, *Physical Review B* **38**, 11322 (1988).
18. W. Y. Ching, Y.-N. Xu, and K. W. Wong, *Physical Review B* **40**, 7684 (1989).
19. J. Ghijsen, L. H. Tjeng, H. Eskes, G. A. Sawatzky, and R. L. Johnson, *Physical Review B* **42**, 2268 (1990).
20. M. Takahashi and J.-I. Igarashi, *Physical Review B* **56**, 12818 (1997).
21. H. Eskes, L. H. Tjeng, and G. A. Sawatzky, *Physical Review B* **41**, 288 (1990).
22. N. F. Mott, *Proceedings of the Royal Society of London Series A* **62**, 416 (1949).
23. J. Zaanen, G. A. Sawatzky, and J. W. Allen, *Physical Review Letters* **55**, 418 (1985).
24. M. A. van Veenendaal and G. A. Sawatzky, *Physical Review Letters* **70**, 2459 (1993).
25. M. A. van Veenendaal, H. Eskes, and G. A. Sawatzky, *Physical Review B* **47**, 11462 (1993).
26. G. van der Laan, C. Westra, C. Haas, and G. A. Sawatzky, *Physical Review B* **23**, 4369 (1981).
27. K. Okada and A. Kotani, *Journal of the Physical Society of Japan* **58**, 2578 (1989).